



Immunization against *Anaplasma phagocytophilum* Adhesin Binding Domains Confers Protection against Infection in the Mouse Model

Waheeda A. Naimi,^a Jacob J. Gumpf,^a Ryan S. Green,^a Jerilyn R. Izac,^{a*} Matthew P. Zellner,^a Daniel H. Conrad,^a Richard T. Marconi,^a Rebecca K. Martin,^a  Jason A. Carlyon^a

^aDepartment of Microbiology and Immunology, Virginia Commonwealth University Medical Center, School of Medicine, Richmond, Virginia, USA

ABSTRACT *Anaplasma phagocytophilum* causes granulocytic anaplasmosis, a debilitating infection that can be fatal in the immunocompromised. It also afflicts animals, including dogs, horses, and sheep. No granulocytic anaplasmosis vaccine exists. Because *A. phagocytophilum* is an obligate intracellular bacterium, inhibiting microbe-host cell interactions that facilitate invasion can disrupt infection. The binding domains of *A. phagocytophilum* adhesins *A. phagocytophilum* invasion protein A (AipA), *A. phagocytophilum* surface protein (Asp14), and outer membrane protein A (OmpA) are essential for optimal bacterial entry into host cells, but their relevance to infection *in vivo* is undefined. In this study, C57BL/6 mice were immunized with a cocktail of keyhole limpet hemocyanin-conjugated peptides corresponding to the AipA, Asp14, and OmpA binding domains in alum followed by challenge with *A. phagocytophilum*. The bacterial peripheral blood burden was pronouncedly reduced in immunized mice compared to controls. Examination of pre- and postchallenge sera from these mice revealed that immunization elicited antibodies against AipA and Asp14 peptides but not OmpA peptide. Nonetheless, pooled sera from pre- and postchallenge groups, but not from control groups, inhibited *A. phagocytophilum* infection of HL-60 cells. Adhesin domain immunization also elicited interferon gamma (IFN- γ)-producing CD8-positive (CD8⁺) T cells. A follow-up study confirmed that immunization against only the AipA or Asp14 binding domain was sufficient to reduce the bacterial peripheral blood load in mice following challenge and elicit antibodies that inhibit *A. phagocytophilum* cellular infection *in vitro*. These data demonstrate that AipA and Asp14 are critical for *A. phagocytophilum* to productively infect mice, and immunization against their binding domains elicits a protective immune response.

KEYWORDS adhesins, *Anaplasma*, vaccine

Granulocytic anaplasmosis is an emerging human and veterinary infection that is primarily transmitted by *Ixodes* species ticks, but it can also be acquired through blood transfusion, perinatally, and possibly by exposure to infected blood (1–8). The disease presents as an acute, nonspecific febrile illness accompanied by chills, headache, malaise, leukopenia, thrombocytopenia, and increased levels of serum transaminases. Potential severe complications include seizures, pneumonitis, rhabdomyolysis, hemorrhage, shock, elevated susceptibility to secondary infection, and death (4, 7). Most human granulocytic anaplasmosis (HGA) cases occur in the upper midwestern and northeastern states, but its geographic range is expanding (9). Moreover, even though nearly 6,000 HGA cases were reported in 2017 (<https://www.cdc.gov/anaplasmosis/stats/index.html>), seroepidemiologic evidence indicates that the actual annual incidence of HGA in the United States is likely considerably

Citation Naimi WA, Gumpf JJ, Green RS, Izac JR, Zellner MP, Conrad DH, Marconi RT, Martin RK, Carlyon JA. 2020. Immunization against *Anaplasma phagocytophilum* adhesin binding domains confers protection against infection in the mouse model. Infect Immun 88:e00106-20. <https://doi.org/10.1128/IAI.00106-20>.

Editor Guy H. Palmer, Washington State University

Copyright © 2020 American Society for Microbiology. All Rights Reserved.

Address correspondence to Jason A. Carlyon, jason.carlyon@vcuhealth.org.

* Present address: Jerilyn R. Izac, Department of Microbial Pathogenesis, University of Maryland School of Dentistry, Baltimore, Maryland, USA.

Received 12 May 2020

Returned for modification 10 June 2020

Accepted 2 July 2020

Accepted manuscript posted online 13 July 2020

Published 18 September 2020

higher (10–15). The disease also occurs in Europe and Asia (4). Granulocytic anaplasmosis resolves when treated with doxycycline, but due to its nonspecific onset, it can be difficult to diagnose at presentation when antibiotic therapy would maximally prevent progression to severe complications (4, 7). Aside from minimizing one's exposure to tick-infested environments, there are no prophylactic measures for HGA, and a vaccine has not been developed.

The etiologic agent of granulocytic anaplasmosis is *Anaplasma phagocytophilum*, an obligate intracellular bacterium that infects neutrophils and bone marrow progenitors (4, 7). *A. phagocytophilum* exhibits a biphasic infection cycle in which it cycles between two morphotypes, an infectious dense-cored (DC) form that binds and induces its own uptake into a host cell-derived vacuole, and a noninfectious reticulate cell form that replicates within the vacuole to yield a bacteria-filled inclusion called a morula (16). Due to its obligatory intracellular nature, adhesins that mediate binding to and invasion of host cells are essential for *A. phagocytophilum* infection and survival. Three *A. phagocytophilum* adhesins that have been identified are outer membrane protein A (OmpA), 14-kDa *A. phagocytophilum* surface protein (Asp14), and *A. phagocytophilum* invasion protein A (AipA) (17–19). All are present on the DC surface and are transcriptionally upregulated during *A. phagocytophilum* host cell entry and during the tick blood meal that transmits the bacterium to mammals (17–19). OmpA engages sialyl-Lewis x and structurally similar α 2,3-sialylated and α 1,3-fucosylated glycans to mediate pathogen binding and entry (18, 20). Asp14 is largely dispensable for cellular adherence but interacts with host cell surface protein disulfide isomerase to exploit the enzyme's thiol reductase activity to induce bacterial invasion (17, 21). Similar to Asp14, AipA minorly contributes to *A. phagocytophilum* adhesion but promotes bacterial uptake via a receptor that remains to be identified (19). The adhesins' functionally essential domains have been delineated as linear stretches of 12 to 18 amino acids corresponding to OmpA residues 59 to 74 (OmpA₅₉₋₇₄), Asp14₁₁₃₋₁₂₄, and AipA₉₋₂₁ (19, 20). Antibodies targeting any one of these domains reduces infection of myeloid host cells *in vitro* by approximately 50%, whereas an antibody cocktail targeting all three impairs infection by approximately 80% (20). The relevance of OmpA₅₉₋₇₄, Asp14₁₁₃₋₁₂₄, and AipA₉₋₂₁ to *A. phagocytophilum* infection *in vivo* is unknown.

In this study, immunization of mice against keyhole limpet hemocyanin (KLH)-conjugated peptides mimicking the OmpA, Asp14, and AipA adhesin domains yielded antibodies against Asp14₁₁₃₋₁₂₄ and AipA₉₋₂₁ that inhibited *A. phagocytophilum* infection of myeloid host cells and protected the mice against the bacterium's ability to establish a productive infection. The observed reduction in pathogen burden in mice was more pronounced than that for tissue culture cells, which is likely attributable, at least in part, to interferon gamma (IFN- γ)-producing CD8-positive (CD8⁺) T cells elicited by the immunization. Subsequent immunization against only Asp14₁₁₃₋₁₂₄ or AipA₉₋₂₁ also achieved partial protection. These findings reveal the importance of the Asp14 and AipA adhesin domains to *A. phagocytophilum* infectivity *in vivo* and signify their potential as protective epitopes.

RESULTS

Immunization of mice against *A. phagocytophilum* adhesin binding domains confers partial protection against infection. To determine if the OmpA₅₉₋₇₄, Asp14₁₁₃₋₁₂₄, and AipA₉₋₂₁ binding domains are important for *A. phagocytophilum* infection *in vivo* and to assess their potential as protective epitopes, C57BL/6 mice were immunized with a cocktail of KLH-conjugated peptides corresponding to each domain in alum. The mice were injected with *A. phagocytophilum* DC organisms, and the resulting bacterial load in the peripheral blood was correlated with the immunization-induced immune responses. Figure 1 presents a schematic overview of the experiment. The five experimental groups, each of which consisted of 10 mice, were (i) no immunization or bacterial challenge, (ii) no immunization followed by *A. phagocytophilum* challenge, (iii) injection with alum followed by *A. phagocytophilum* challenge, (iv) injection with KLH and alum followed by *A. phagocytophilum* challenge, and (v) injection with KLH-adhesin domain peptide cocktail in alum

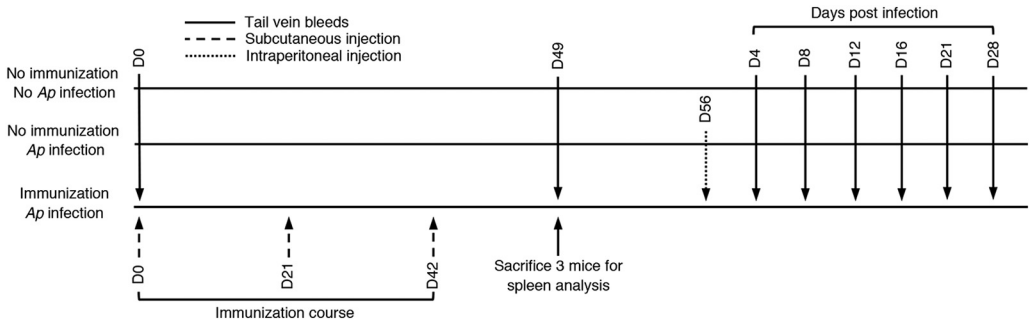


FIG 1 Experimental overview. Ten C57BL/6 mice per group were bled on day 0, and preimmune sera were collected. Immunized mice received their first immunization via subcutaneous (s.c.) shoulder injection and two boosts on days 21 and 42. All mice were bled on day 49, and sera were collected to check for the presence of peptide-specific antibodies by ELISA. Also on day 49, three mice from each group were sacrificed by cardiac puncture, and spleens were harvested for further analysis via flow cytometry and T-cell restimulation. The remaining seven mice were challenged interperitoneally (i.p.) with 1×10^8 *A. phagocytophilum* (Ap) organisms on day 56. Mice were bled on days 4, 8, 12, 16, and 21 and sacrificed on day 28. DNA isolations and peripheral blood smears were used to analyze bacterial load via qPCR and microscopically examined for neutrophils that contained morulae, respectively.

followed by *A. phagocytophilum* challenge (Table 1). The mice were boosted on days 21 and 42. On day 49, serum samples and spleens were recovered from all 10 and 3 mice per group, respectively. On day 56, the remaining seven mice per group were intraperitoneally injected with *A. phagocytophilum* DC organisms followed by assessment of the bacterial peripheral blood burden using quantitative PCR (qPCR) and examination of blood smears for the percentage of neutrophils harboring morulae. The *A. phagocytophilum* burden peaked by day 12 and subsided to undetectable levels by day 28 in all mice that had been inoculated (Fig. 2). Notably, however, both the *A. phagocytophilum* DNA load and percentage of neutrophils containing morulae were pronouncedly reduced in mice that had been immunized with the KLH-adhesin peptide domain cocktail compared to the three infected control groups. For instance, on day 12, the bacterial DNA load and number of infected neutrophils were reduced by as much as 4.5- and 4.9-fold, respectively, in peptide cocktail-immunized mice.

Asp14₁₁₃₋₁₂₄ and AipA₉₋₂₁ induce antibodies that inhibit bacterial infection of host cells. To evaluate if the immunization procedure elicited antibodies specific for the cognate antigens, day 49 prechallenge serum was used to screen enzyme-linked immunosorbent assay (ELISA) plates that had been coated with KLH alone or unconjugated OmpA₂₃₋₄₀, OmpA₅₉₋₇₄, Asp14₁₁₃₋₁₂₄, or AipA₉₋₂₁ peptide. OmpA₂₃₋₄₀ served as a negative control because it had not been used as an immunogen and plays no role in *A. phagocytophilum* infection (20). Screening the plates with rabbit antisera specific for each peptide or KLH alone verified that the plates had been properly coated with each antigen (Fig. 3). Sera from mice that had been injected with KLH or KLH-conjugated peptides recognized KLH (Fig. 3A). Sera from peptide cocktail-immunized mice detected unconjugated Asp14₁₁₃₋₁₂₄ and AipA₉₋₂₁ peptides, but neither OmpA₅₉₋₇₄ nor OmpA₂₃₋₄₀ (Fig. 3B to E). Serum samples from the four control groups

TABLE 1 Experimental groups used in immunization

Group ^a	Immunization	Peptide(s)	Infection ^b
1	No immunization	N/A	No
2	No immunization	N/A	Yes
3	Adjuvant only	N/A	Yes
4	KLH plus adjuvant	N/A	Yes
5	KLH-conjugated peptide plus adjuvant	OmpA ₅₉₋₇₄ , Asp14 ₁₁₃₋₁₂₄ , AipA ₉₋₂₁	Yes
6	KLH-conjugated peptide plus adjuvant	Asp14 ₁₁₃₋₁₂₄	Yes
7	KLH-conjugated peptide plus adjuvant	AipA ₉₋₂₁	Yes

^aMouse immunization study 1 consists of groups 1 to 5. Mouse experiment 2 consists of groups 1 to 4, 6, and 7.

^bMice were challenged interperitoneally with 1×10^8 *A. phagocytophilum* organisms on day 56.

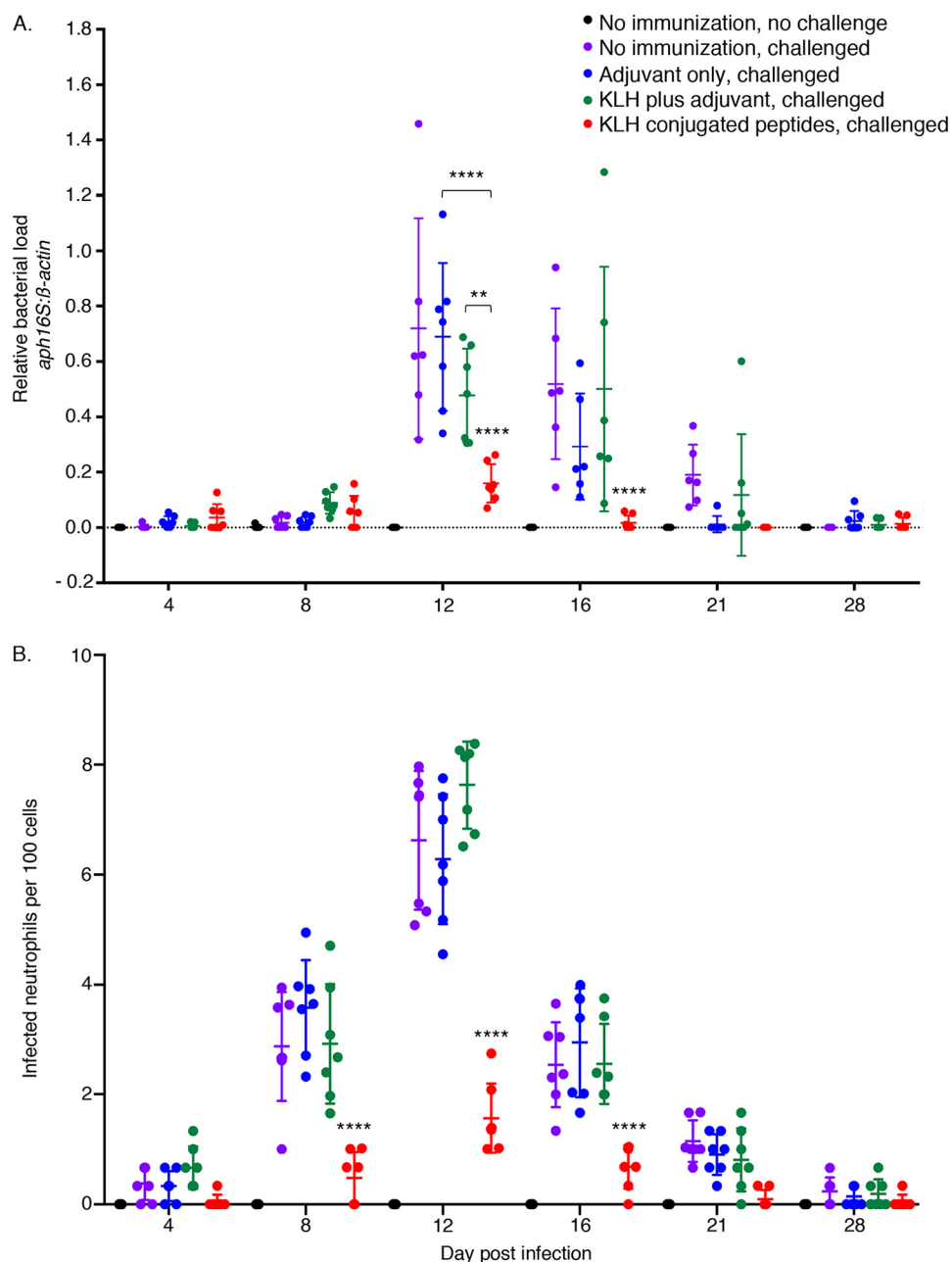


FIG 2 Mice immunized against an adhesin domain peptide cocktail are resistant to *A. phagocytophilum* infection. C57BL/6 mice that had been immunized against a cocktail of KLH-conjugated OmpA₅₉₋₇₄, Asp14₁₁₃₋₁₂₄, and AipA₉₋₂₁ or mice of the indicated control groups were infected with *A. phagocytophilum* DC organisms. (A) Peripheral blood drawn on the indicated days postinfection was analyzed by qPCR using gene-specific primers. Relative *A. phagocytophilum* 16S rRNA genes (*aph16S*) to murine β -actin DNA levels were determined using the $2^{-\Delta\Delta CT}$ method. (B) Peripheral blood samples were also examined by light microscopy for ApV-containing neutrophils. Each symbol corresponds to the percentage of *A. phagocytophilum*-infected neutrophils as determined by examining at least 100 neutrophils per mouse. Data are the mean \pm standard deviation (SD) of the percentages determined for seven mice per group. Error bars indicate standard deviation among the samples per time point. Statistically significant values are indicated. ** $P < 0.01$; **** $P < 0.0001$.

that had not been immunized against the peptide cocktail failed to recognize any peptide. Next, pre- or postchallenge sera from all mice per group were pooled and examined for the ability to inhibit *A. phagocytophilum* infection of promyelocytic HL-60 cells. Only sera from the KLH-peptide-immunized mice significantly reduced the percentage of infected cells and the number of *A. phagocytophilum*-occupied vacuoles

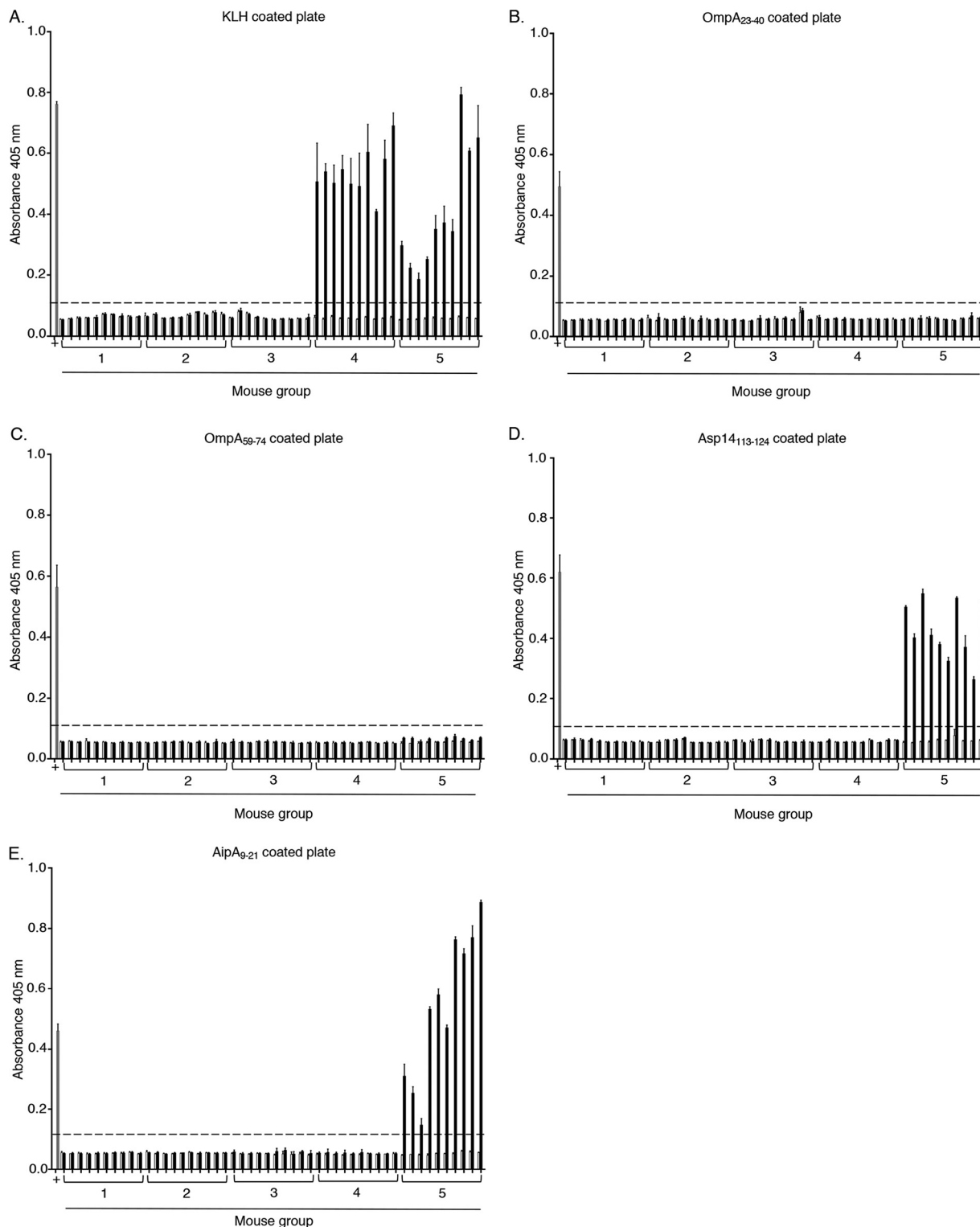


FIG 3 Immunization of mice against OmpA, Asp14, and AipA adhesin domains elicits antibodies against Asp14₁₁₃₋₁₂₄ and AipA₉₋₂₁ but not OmpA₅₉₋₇₄. Preimmune sera (white bars) and sera collected on day 49 (black bars) were added to wells that had been coated with KLH (A) or unconjugated peptides corresponding to OmpA₂₃₋₄₀ (B), OmpA₅₉₋₇₄ (C), Asp14₁₁₃₋₁₂₄ (D), and AipA₉₋₂₁ (E). All sera were analyzed in triplicate via ELISA. To verify that the wells had been properly coated with each antigen of interest, positive-control wells (+) were screened with rabbit antisera specific for each antigen (gray bars). Absorbance was read at 405 nm 30 postaddition of chromogenic substrate. The dotted line in each panel indicates two times the absorbance value obtained using preimmune serum.

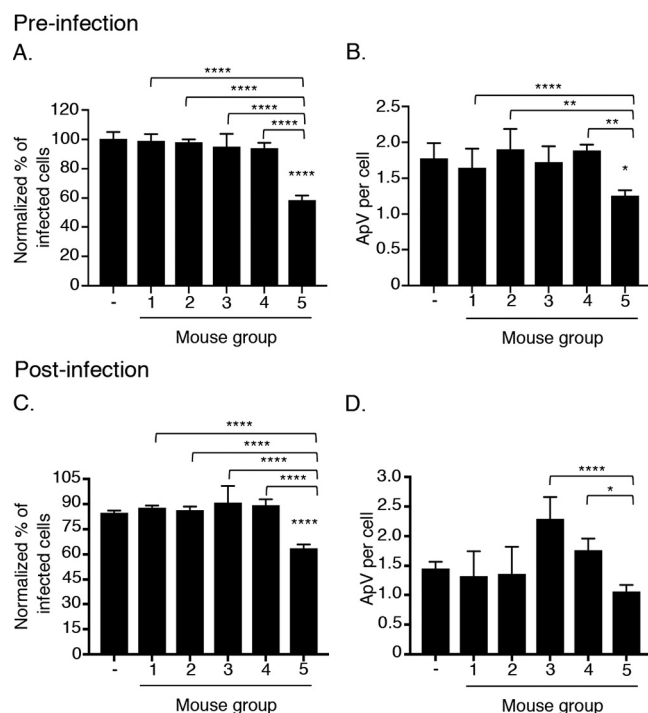


FIG 4 Pre- and postchallenge sera from mice immunized against adhesin domains inhibit *A. phagocytophilum* infection of host cells. *A. phagocytophilum* bacteria were treated with pooled day 0 preimmune sera (–) or pooled sera collected on day 49 (prechallenge) (A and B) or day 84 (28 days postchallenge) (C and D) at a 1:5 dilution. Treated bacteria were incubated with HL-60 cells for 1 h. At 24 h, the cells were examined by immunofluorescence microscopy for the percentage of infected cells (A and C) and number of ApVs per cell (B and D). Data are presented as the mean \pm SD of triplicate samples. Statistically significant values relative to preimmune serum-treated cells are indicated by asterisks without brackets. Statistically significant values among the five groups are indicated by asterisks with brackets. * $P < 0.05$; ** $P < 0.01$; *** $P < 0.0001$.

(ApVs) per cell (Fig. 4). Specifically, pre- and postchallenge sera recovered from peptide immunized mice reduced infection by 41.7% and 25.0% and lowered the number of ApVs per cell by 52.0% and 40.0%, respectively. These data establish that immunization of mice against KLH-conjugated peptides mimicking the OmpA, Asp14, and AipA adhesin domains specifically elicited antibodies against Asp14₁₁₃₋₁₂₄ and AipA₉₋₂₁, but not OmpA₅₉₋₇₄, and that said antibodies inhibit *A. phagocytophilum* infection of myeloid host cells.

Immunization of mice against the adhesin domains elicits IFN- γ -producing CD8⁺ T cells. To assess the T-cell responses elicited by immunization, splenocytes from three mice per group were recovered on day 49, pooled, and examined by flow cytometry. Minor statistically significant reductions in the overall percentage of live CD8⁺ T cells were observed for the adjuvant-only and KLH-peptide cocktail plus adjuvant groups (Fig. 5A). No statistically significant difference in the percentage of live CD4⁺ T cells was observed (Fig. 5C). The T-cell population was labeled with tracer dye, restimulated with unconjugated adhesin domain peptide cocktail, and examined for IFN- γ production. A significant increase was observed in the percentage of IFN- γ -positive CD8⁺ T cells from the spleens of KLH-adhesin peptide domain cocktail-immunized mice versus those of the no-immunization and alum-alone control groups (Fig. 5B). No difference was observed for IFN- γ -producing CD4⁺ T cells among the groups (Fig. 5D). The lack of change in the percentage of live CD4⁺ cells correlates with the lack of change in the percentage of IFN- γ -positive CD4⁺ T cells. The reduction in viable CD8⁺ T cells in peptide-immunized mice potentially correlates with their being utilized to combat infection. These data confirm that immunization with OmpA₅₉₋₇₄, Asp14₁₁₃₋₁₂₄, and/or AipA₉₋₂₁ elicits a CD8⁺ T-cell response.

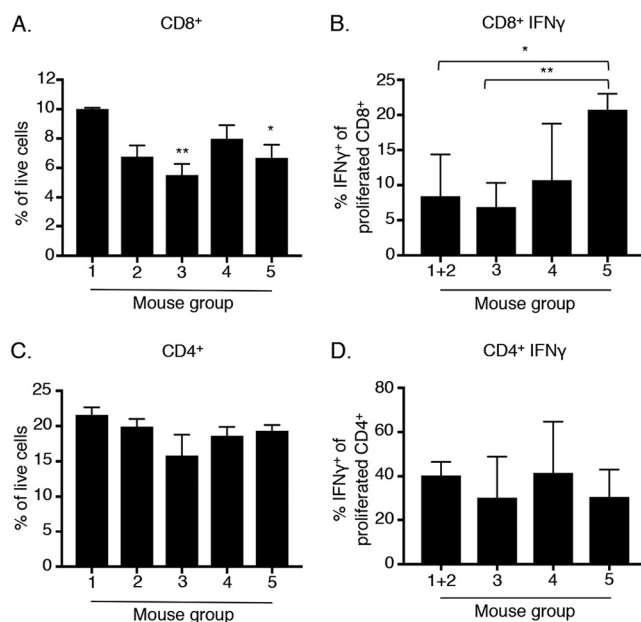


FIG 5 Immunization of mice against the adhesin domains elicits IFN- γ -producing CD8⁺ T cells. Pooled splenocytes recovered from three mice per group were on day 49 prior to bacterial challenge were assessed by flow cytometry to calculate the percentage of live CD8⁺ and CD4⁺ T cells (A and C). CD8⁺ (B) and CD4⁺ T cells (D) from the pooled splenocytes were labeled with cell tracer dye, restimulated with the unconjugated adhesin domain peptide cocktail for 3 days, and examined for intracellular IFN- γ production by flow cytometry. The mouse group numbers 1 to 5 in each panel are defined as (1) no immunization or bacterial challenge, (2) no immunization followed by *A. phagocytophilum* challenge, (3) injection with alum followed by *A. phagocytophilum* challenge, (4) injection with KLH and alum followed by *A. phagocytophilum* challenge, and (5) injection with KLH-adhesin domain peptide cocktail in alum followed by *A. phagocytophilum* challenge. Please note that in panels B and D, splenocytes from nonimmunized groups 1 and 2 were pooled. Statistically significant values are indicated. * $P < 0.05$; ** $P < 0.01$.

Immunization of mice against Asp14₁₁₃₋₁₂₄ or AipA₉₋₂₁ is sufficient to confer partial protection against *A. phagocytophilum* infection via blocking antibodies.

Because mice that developed immune responses against both KLH-Asp14₁₁₃₋₁₂₄ and KLH-AipA₉₋₂₁ were recalcitrant to *A. phagocytophilum* infection, it was examined if immunization against either individual antigen is sufficient to confer protection. The immunization experiment was repeated with the same four control groups (designated 1 to 4) plus groups that were injected with either KLH-conjugated Asp14₁₁₃₋₁₂₄ (group 6) or AipA₉₋₂₁ (group 7) in alum (Table 1). Immunization against either epitope was adequate to significantly reduce the *A. phagocytophilum* burden following challenge, and the partial protection observed for KLH-Asp14₁₁₃₋₁₂₄-immunized mice was greater than that observed for KLH-AipA₉₋₂₁-immunized mice (Fig. 6). Specifically, maximal reductions of 6.5-fold and 2.7-fold were observed for the bacterial DNA load on day 12 and the number of infected neutrophils on day 8, respectively, in KLH-Asp14₁₁₃₋₁₂₄-immunized mice. For KLH-AipA₉₋₂₁-immunized mice, the *A. phagocytophilum* DNA burden was lowered by as much as 4.5-fold, and the number of infected neutrophils by as much as 1.9-fold, both of which were observed on day 8. Immunization with KLH-Asp14₁₁₃₋₁₂₄ or KLH-AipA₉₋₂₁ elicited antibodies that specifically recognized their respective antigen and reduced infection of HL-60 cells by approximately 50% to 55% (Fig. 7). Unfortunately, due to a technical error, three KLH-AipA₉₋₂₁-immunized mice died prior to bacterial challenge. Consequently, mice could not be sacrificed for CD4⁺ and CD8⁺ splenocyte analyses to allow for assessment of the bacterial load in at least seven mice per group. Regardless, these data allow for the conclusion that the Asp14 and AipA binding domains are each important for *A. phagocytophilum* to establish a productive infection in mice and validate that both are protective B-cell epitopes.

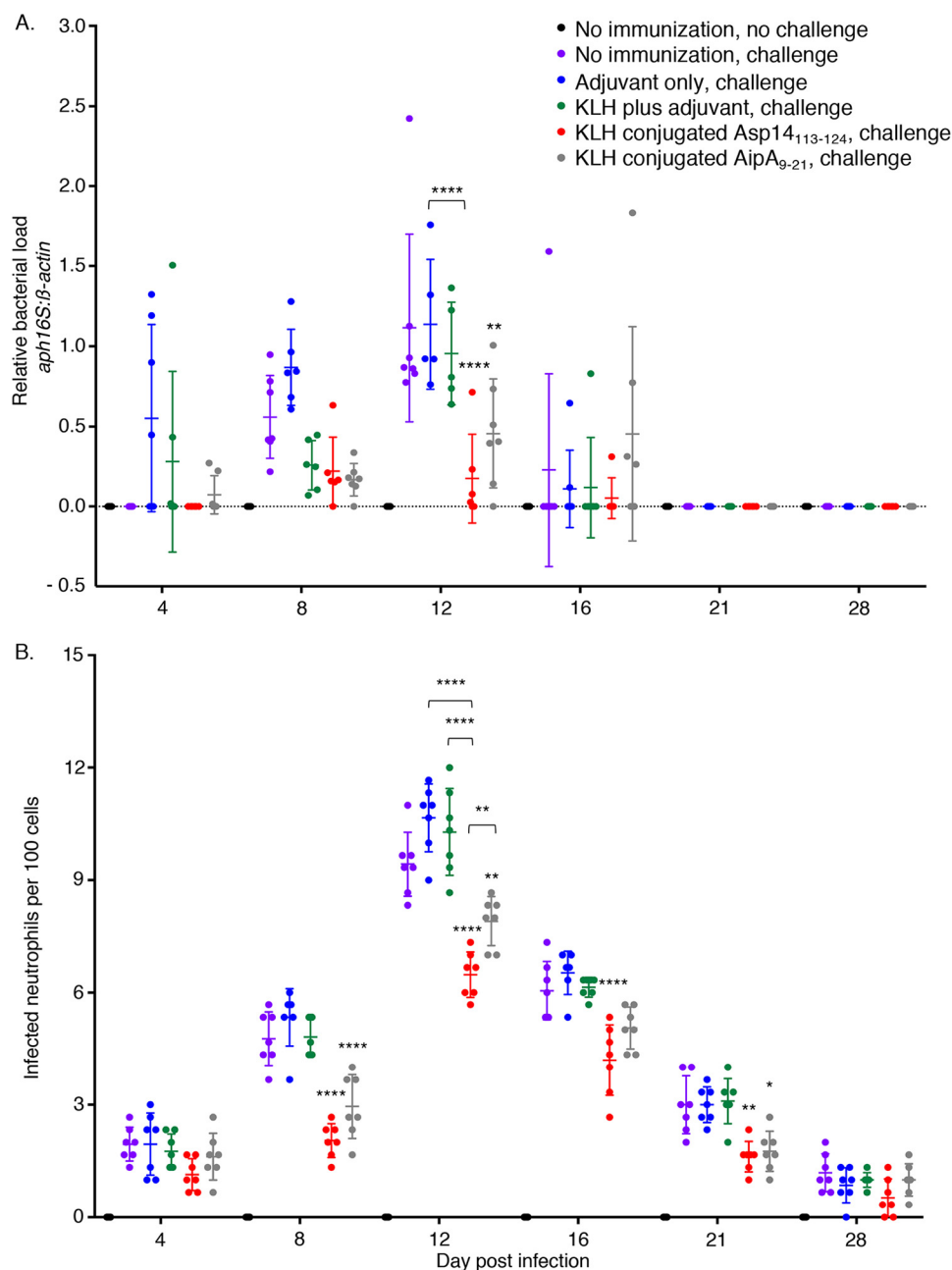


FIG 6 Mice immunized against Asp14₁₁₃₋₁₂₄ or AipA₉₋₂₁ are resistant to *A. phagocytophilum* infection. C57BL/6 mice that had been immunized against KLH-Asp14₁₁₃₋₁₂₄ or KLH-AipA₉₋₂₁ or mice of the indicated control groups were inoculated with *A. phagocytophilum* DC bacteria. (A) Peripheral blood drawn on the indicated days postinfection was analyzed by qPCR using gene-specific primers. Relative *A. phagocytophilum* 16S rRNA genes (*aph16S*) to murine β -actin DNA levels were determined using the $2^{-\Delta\Delta CT}$ method. (B) Peripheral blood samples were also examined by light microscopy for ApV-containing neutrophils. Each symbol corresponds to the percentage of *A. phagocytophilum*-infected neutrophils as determined by examining at least 100 neutrophils per mouse. Data are the mean \pm SD of the percentages determined for seven mice per group. Error bars indicate standard deviation among the samples per time point. Statistically significant values are indicated. * $P < 0.05$; ** $P < 0.01$; **** $P < 0.0001$.

DISCUSSION

As an obligate intracellular bacterium, *A. phagocytophilum* must invade neutrophils to survive. Whereas its infectivity for myeloid host cells *in vitro* is known to rely, at least in part, on the Asp14₁₁₃₋₁₂₄, AipA₉₋₂₁, and OmpA₅₉₋₇₄ receptor binding domains (19, 20), these linear determinants' relevance to *A. phagocytophilum* infection *in vivo* was

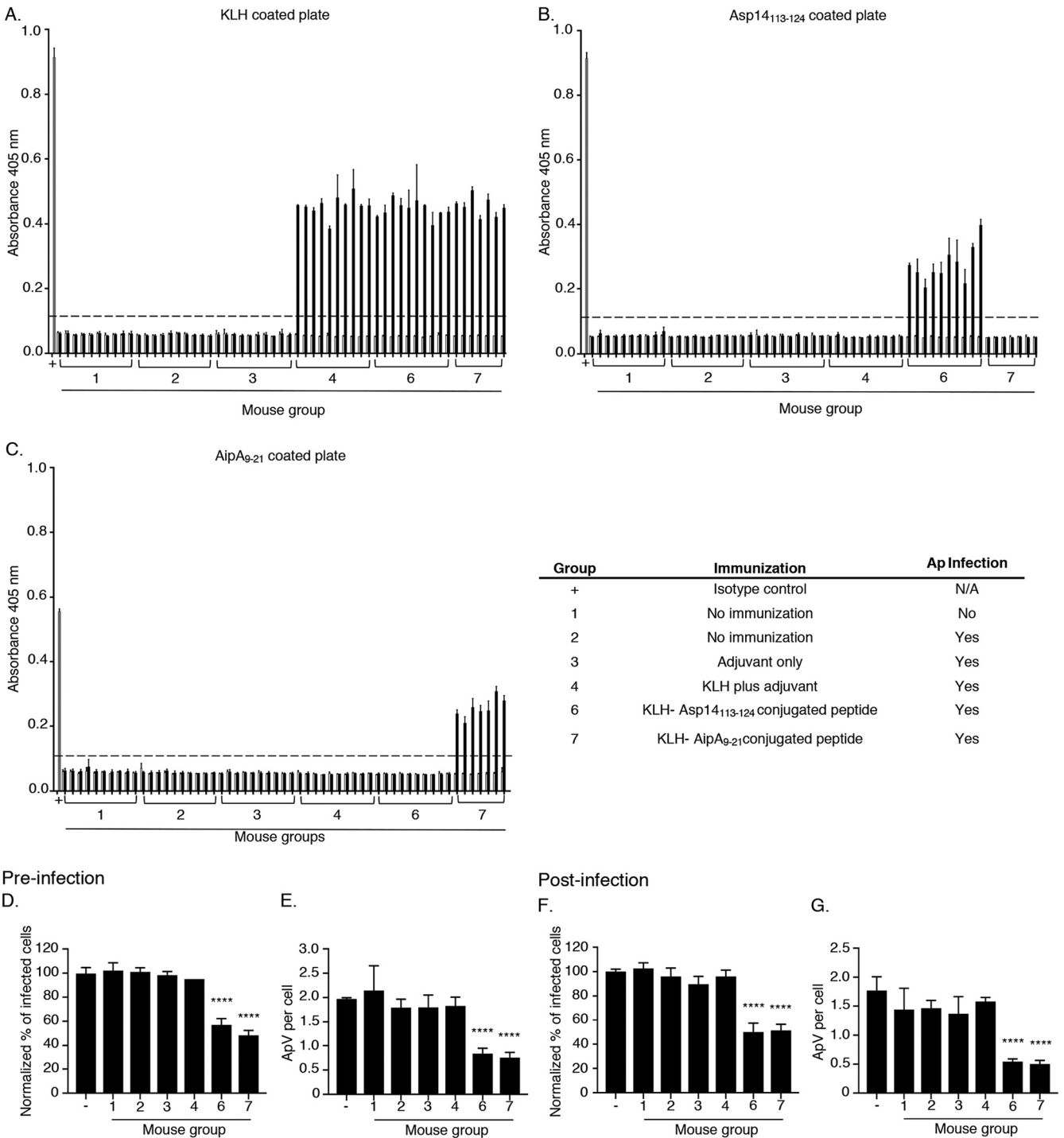


FIG 7 Immunization against Asp14₁₁₃₋₁₂₄ or AipA₉₋₂₁ elicits antigen-specific antibodies that inhibit *A. phagocytophilum* infection of host cells. (A to C) Immunization against Asp14₁₁₃₋₁₂₄ or AipA₉₋₂₁ peptide elicits antigen-specific antibodies. Preimmune sera (white bars) and sera collected on day 49 (black bars) were added to wells that had been coated with KLH (A), unconjugated Asp14₁₁₃₋₁₂₄ (B), or AipA₉₋₂₁ peptide (C). All sera were analyzed in triplicate via ELISA. To verify that the wells had been coated with each antigen of interest, positive-control wells (+) were screened with rabbit antisera specific for each antigen (gray bars). Absorbance was read at 405 nm 30 postaddition of chromogenic substrate. The dotted line in each panel indicates twice the absorbance value obtained using preimmune serum. (D to G) Pre- and postchallenge sera from mice immunized against Asp14₁₁₃₋₁₂₄ or AipA₉₋₂₁ inhibit *A. phagocytophilum* infection of host cells. *A. phagocytophilum* DC organisms were treated with pooled day 0 preimmune sera (–) or pooled sera collected on day 49 (prechallenge) (D and E) or day 84 (28 days postchallenge) (F and G) at a 1:5 dilution. Treated bacteria were incubated with HL-60 cells for 1 h. At 24 h, the cells were examined by immunofluorescence microscopy for the percentage of infected cells (D and F) and number of ApVs per cell (E and G). Data are presented as the mean \pm SD of triplicate samples. Preimmune and experimental groups were normalized to a no-sera control. Statistically significant values relative to preimmune serum treated cells are indicated. ****, $P < 0.0001$.

unknown. This study demonstrates that at least Asp14₁₁₃₋₁₂₄ and AipA₉₋₂₁ are critical for *A. phagocytophilum* productive infection in mice. Animals immunized against a cocktail of KLH-conjugated peptides corresponding to the three domains in alum exhibited significantly reduced *A. phagocytophilum* 16S rRNA gene loads and infected neutrophils in peripheral blood compared to controls. The observed reduction in pathogen burden correlated with the presence of antibodies specific for Asp14₁₁₃₋₁₂₄ and AipA₉₋₂₁ but not OmpA₅₉₋₇₄ in sera from KLH-peptide cocktail-immunized mice. KLH-OmpA₅₉₋₇₄ fails to elicit an antibody response when administered in alum but does so when provided in a Freund's adjuvant-based immunization protocol (20), which suggests that it is poorly immunogenic. Indeed, we previously observed that *A. phagocytophilum* infection does not yield a strong humoral immune response against full-length OmpA (18). Also, an evaluation of the efficacy of *Anaplasma marginale* outer membrane proteins as potential vaccinogens found its OmpA homolog, AM854, to be a subdominant antigen (22, 23).

The reduction in bacterial load in adhesin domain peptide cocktail-immunized mice following challenge with *A. phagocytophilum* was much greater than that observed when pooled sera from these mice were assessed for the ability to inhibit infection of HL-60 cells. The immunization likely elicited additional nonblocking antibody responses that contributed to controlling the infection *in vivo*. Opsonization of *A. phagocytophilum* DCs by Asp14₁₁₃₋₁₂₄ and AipA₉₋₂₁ antibodies could have led to their destruction by complement-mediated killing and/or lysosomal targeting due to Fc receptor (FcR)-mediated phagocytosis, the latter of which has been observed for antibodies that protect against other intracellular bacteria (24). Another contributing factor could have been IFN- γ produced by CD8⁺ T cells. IFN- γ helps control *A. phagocytophilum* early in infection, presumably by promoting macrophage-mediated intracellular killing (25–29). CD8⁺ T, NK, and NKT cells are functionally impaired in mice experimentally infected with the bacterium, as all three cell types produce IFN- γ when exposed to *A. phagocytophilum*-loaded dendritic cells *ex vivo*, and ionomycin-stimulated CD8⁺ T cells are defective for degranulation (30, 31). Perhaps the elicitation of IFN- γ -producing CD8⁺ T cells offsets the cytotoxic failure of this cell type that *A. phagocytophilum* infection normally induces. A CD4⁺ T-cell response, which is most critical for controlling granulocytic anaplasmosis (26), was not induced by the immunization.

Immunization against Asp14₁₁₃₋₁₂₄ or AipA₉₋₂₁ was sufficient to achieve partial protection that was comparable to that induced by the peptide cocktail. However, the reduction in bacterial load in Asp14₁₁₃₋₁₂₄-immunized mice was significantly greater than in mice immunized against AipA₉₋₂₁. These data are consistent with prior observations that antiserum targeting the Asp14 binding domain more effectively inhibits *A. phagocytophilum* infection of host cells than antiserum against the AipA binding domain (19, 20). Asp14₁₁₃₋₁₂₄ antibodies presumably block infection *in vivo* by antagonizing interaction of the adhesin's K122 and E123 with protein disulfide isomerase (PDI), which is a critical step in cellular invasion (21). In support of this premise, the inefficiency of *A. phagocytophilum* to establish productive infections in Asp14₁₁₃₋₁₂₄-immunized mice and conditional knockout mice lacking myeloid expression of PDI is similar (21). Whereas the specific contribution of the interaction between AipA and its receptor provides to *A. phagocytophilum* cellular entry is undefined, the current study and the PDI conditional knockout mouse study (21) together suggest that, relative to AipA, Asp14 plays a predominant role in *A. phagocytophilum* infection *in vivo*. The results of this mouse study differ from our previous report that demonstrated that OmpA₅₉₋₇₄, Asp14₁₁₃₋₁₂₄, and AipA₉₋₂₁ antibodies together synergistically block *A. phagocytophilum* infection of host cells *in vitro* significantly better than any of the antibodies individually or in pairs (20). This distinction is likely due to the additional effects of CD8⁺ T cells and opsonization-induced bacterial killing *in vivo* and/or relative differences that Asp14 and AipA play during *A. phagocytophilum* infection in mammals versus host cells *in vitro*.

In addition to validating the importance of Asp14 and AipA to *A. phagocytophilum* infection *in vivo*, this study substantiates these adhesins' binding domains as protective

antigens. Immunizing against Asp14₁₁₃₋₁₂₄ and AipA₉₋₂₁ in alum, an adjuvant that is approved for human and veterinary vaccines (32), elicits a partially protective immune response that reduces the *A. phagocytophilum* load 4- to 5-fold. KLH-conjugated peptides are not suitable for FDA- or USDA-approved vaccines. However, the data herein indicate the benefit of including Asp14₁₁₃₋₁₂₄ and AipA₉₋₂₁ sequences as part of a larger protective antigen such as a chimeritope. Chimeritopes are laboratory-designed recombinant polypeptides that harbor multiple isolated epitopes or critical functional domains derived from one or more proteins or protein variants. This combined epitope strategy has advantages over the delivery of antigen cocktails in that regions of natural antigens that are reactogenic or that elicit nonprotective antibody responses can be excluded. Marconi and colleagues successfully used this method to develop a *Borrelia burgdorferi* outer surface protein C-based chimeritope vaccine antigen for canine Lyme disease (33–38), which is commercially available as Vanguard-crLyme. Accordingly, development of a chimeritope that minimally includes Asp14₁₁₃₋₁₂₄ and AipA₉₋₂₁ should be considered. Reevaluating OmpA₅₉₋₇₄ in this context is warranted because of its critical role in bacterial docking to the host cell surface and since presenting this determinant as part of a larger immunogenic polypeptide could enhance its antigenicity to generate a protective response against all three domains of interest. Moving forward, as Asp14₁₂₃₋₁₂₄ and/or AipA₉₋₂₁ elicit IFN- γ and this cytokine is associated with inflammatory hepatic histopathologic injury in *A. phagocytophilum* infections (27, 39–42), it will be prudent to evaluate mice immunized against these antigens for histopathology. Overall, this report advances understanding of *A. phagocytophilum*-host interactions *in vivo* that are critical for productive infection and establishes a direction toward the development of a granulocytic anaplasmosis vaccine.

MATERIALS AND METHODS

Cultivation of uninfected and *A. phagocytophilum*-infected cells, antibodies, and reagents.

Uninfected and *A. phagocytophilum* str. NCH-1-infected human promyelocytic HL-60 cells (ATCC CCL-240; American Type Culture Collection [ATCC], Manassas, VA) were cultivated exactly as described (43). Rabbit-monospecific antisera against KLH-conjugated peptides corresponding to AipA₉₋₂₁, Asp14₁₁₃₋₁₂₄, OmpA₂₃₋₄₀, and OmpA₅₉₋₇₄ were generated as previously described (19, 20). Unconjugated versions of the four peptides were generated by New England Peptide (Gardner, MA). Commercial antibodies used in this study were rabbit anti-hemocyanin (Sigma-Aldrich, St. Louis, MO), Alexa fluorochrome 488-conjugated goat anti-mouse IgG and goat anti-rabbit IgG (Invitrogen, Waltham, MA), horseradish peroxidase (HRP)-conjugated goat anti-mouse IgG, and anti-rabbit IgG (Cell Signaling Technology, Danvers, MA).

Mouse studies. All mouse research was conducted under the approval of the Institutional Animal Care and Use Committee at Virginia Commonwealth University (protocol number AM10220). Immunization experiments were performed with male C57BL/6 mice (Jackson Laboratories, Bar Harbor, ME) because they exhibit greater susceptibility to *A. phagocytophilum* infection than female mice (44). Each experiment used groups of 10 mice that were injected with immunogen or control in a final volume of 200 μ l. On day 0, the mice were bled and sera collected as previously described (45). Also on day 0, the appropriate groups as defined in Table 1 received subcutaneous shoulder injections of adjuvant alone, KLH plus adjuvant, or KLH-conjugated peptides plus adjuvant. Sterile phosphate-buffered saline (PBS) was used as a mock inoculum to inject negative-control animals. Mice that received adjuvant only were injected with alum-based Imject adjuvant (Thermo Fisher). Mice in the KLH plus alum group received 100 μ g of KLH (Thermo Fisher Scientific) in Imject. Each mouse that was injected with KLH-conjugated peptides received 33.3 μ g each of KLH-OmpA₅₉₋₇₄, KLH-Asp14₁₁₃₋₁₂₄, and KLH-AipA₉₋₂₁ or 100 μ g of KLH-Asp14₁₁₃₋₁₂₄ or KLH-AipA₉₋₂₁ in Imject. All mice except for the no-immunization controls received boosts on days 21 and 42. On day 49, blood was collected from the tail vein and sera isolated for indirect ELISA. Also on day 49, three mice per group were euthanized, their blood collected via cardiac puncture, and spleens harvested for flow cytometry and T-cell restimulation assays. On day 56, with the exception of the no-infection controls, all mice were intraperitoneally inoculated with 1×10^8 *A. phagocytophilum* DC organisms as previously described (44). Sterile PBS was used as a mock inoculum to inject negative-control animals. All mice were tail bled on days 4, 8, 12, 16, and 21. On day 28, the mice were euthanized and blood collected by cardiac puncture. Heparin (Sigma-Aldrich) at 100 U ml⁻¹ was added to blood samples collected on days 4, 8, 12, 16, 21, and 28 postinfection. The peripheral blood *A. phagocytophilum* load was analyzed via qPCR and microscopic examination of blood smears for the presence of infected neutrophils as previously described (44).

ELISA. Ninety-six-well plates were coated with 500 ng of KLH or unconjugated peptide per well in carbonate buffer (15 mM sodium carbonate, 24.9 mM sodium bicarbonate, pH 9.6) overnight at 4°C followed by blocking with 5% nonfat dry milk in PBS with 0.2% Tween 20 (PBST) for 3 h at room temperature. The plates were then incubated with the appropriate mouse or rabbit serum at a 1:100 dilution in 5% (vol/vol) nonfat dry milk in PBST for 1 h at room temperature, washed three times with

PBST, incubated with HRP-conjugated anti-mouse or anti-rabbit IgG at a 1:15,000 dilution at room temperature, and washed again. ABTS [2, 2'-azino-bis(3-ethylbenzothiazoline-6-sulfonic acid) diammonium salt] substrate (Sigma-Aldrich, St. Louis, MO) was added at a 1:25,000 dilution in the presence of citrate buffer (10.4 mM citric acid, pH 4.1) and 30% (vol/vol) hydrogen peroxide (Sigma-Aldrich) for 30 min followed by absorbance reading at 405 nm in an ELx 808 plate reader (Fisher Scientific, Hanover Park, IL).

qPCR. DNA was isolated from heparin-treated blood with the DNeasy blood and tissue kit (Qiagen, Germantown, MD). Three DNeasy collections were performed per mouse utilizing 50 μ l of blood per bleed. All three DNA samples per mouse were analyzed by qPCR in triplicate using previously described thermal cycling conditions (43) and primers specific for *A. phagocytophilum* 16S rRNA genes and β -actin (46). Relative 16S rRNA genes levels were normalized to β -actin levels using the cycle threshold ($2^{-\Delta\Delta CT}$) (Livak) method (47) CFX Maestro software (Bio-Rad, Hercules, CA).

A. phagocytophilum cellular infection assay. All preimmune sera were pooled and utilized as a negative control. Five-microliter serum samples from each mouse per group collected on day 49 were pooled and heat inactivated in a 56°C water bath for 30 min. The same was performed for serum samples collected on day 84, which corresponds to day 28 postinfection. To assess the ability of each pooled sera to inhibit *A. phagocytophilum* infection of host cells, DC bacteria from 1.0×10^6 heavily infected ($\geq 90\%$) HL-60 cells were prepared as described previously (16) and resuspended in 20 μ l of Iscove's modified Dulbecco's medium containing 10% (vol/vol) heat-inactivated fetal bovine serum (Gemini Bio-Products, Sacramento, CA) for each infection assay. We added 5 μ l of pooled sera to each bacterial suspension to achieve a final 1:5 dilution. Following 1 h of incubation at 37°C, the HL-60 cells were washed and the synchronous infection allowed to proceed as described (16). At 24 h, aliquots were removed, fixed, and assessed for infection as previously described (48). To account for minor differences in the percentage of infected cells among replicates, values for cells that had been treated with sera were divided by those for untreated cells. The quotient was multiplied by 100 to generate the normalized percentage of infected cells.

Flow cytometry. Spleens were rubbed between two glass slides to yield single-cell suspensions followed by removal of red blood cells using ACK lysing buffer (Quality Biological, Gaithersburg, MD). Splenocytes were stained with fixable Zombie Aqua or Zombie Green (BioLegend, San Diego, CA) per the manufacturer's instructions. Samples were then Fc blocked with 2.4G2 (BD Biosciences, San Jose, CA) for 5 min and stained for 30 min on ice. Flow samples that included multiple Brilliant Violet antibodies were stained in the presence of Brilliant stain buffer (BD Biosciences) per the manufacturer's instructions. All cells were then fixed in 4% paraformaldehyde (PFA) fixation buffer (BioLegend) for 15 min at room temperature. For intracellular cytokine staining, fixed cells were permeabilized with PermWash buffer (BioLegend) per the manufacturer's instructions. Flow data were collected using a BD LSRFortessa running BD FACSDiva 8.0 software, analyzed with FlowJo software version 10.4.2 (FlowJo, Ashland, OR), and graphed using the Prism 7.0 software package (GraphPad, San Diego, CA, USA) on GraphPad Prism. Antibodies utilized for flow cytometry studies were anti-mouse CD45 (clone 30 F11) conjugated to APC/Fire 750 (BioLegend), anti-mouse T-cell receptor beta (TCR β) (clone H57 597) conjugated to Alexa Fluor 700 or PE (BioLegend), anti-mouse CD4 (clone GK1.5) conjugated to BV711 (BioLegend), anti-mouse CD8 (clone 53-6.7) conjugated to PE/Dazzle 594 (BioLegend), anti-mouse IFN- γ (clone XMG1.2) conjugated to Alexa Fluor 647 (BioLegend), and anti-mouse B220 (clone RA3-6B2) conjugated to BUV395 (BD Biosciences). For *ex vivo* stimulation, 5×10^6 splenocytes were plated at 1×10^6 cells ml^{-1} in U-bottom cell culture plates for peptide restimulation with 5 $\mu\text{g ml}^{-1}$ of the unconjugated peptide cocktail used for immunization for 3 days. Prior to plating, cells were labeled with Tag-It Violet (BioLegend). Gating for cell populations was defined as follows: CD8 $^+$ T cells (Zombie-CD45 $^+$ B220 $^-$ TCR β^+ CD4 $^-$ CD8 $^+$), CD4 $^+$ T cells (Zombie-CD45 $^+$ B220 $^-$ TCR β^+ CD4 $^+$ CD8 $^-$), peptide-restimulated IFN- γ^+ CD8 $^+$ T cells (Tag-It Violet $^{\text{low}}$ Zombie-CD45 $^+$ TCR β^+ CD4 $^-$ CD8 $^+$), peptide-restimulated IFN- γ^+ CD4 $^+$ T cells (Tag-It Violet $^{\text{low}}$ Zombie-CD45 $^+$ TCR β^+ CD4 $^+$ CD8 $^-$).

Statistical analyses. Statistical analyses were performed using the Prism 7.0 software package (GraphPad, San Diego, CA, USA). Two-way analysis of variance (ANOVA) with Tukey's *post hoc* test was used to test for a significant difference among groups in all experiments except for data generated by the T-cell restimulation assay, for which a paired Student's *t* test was used to test for statistical significance between paired data. Statistical significance was set at *P* values of <0.05 .

ACKNOWLEDGMENTS

This work was supported by NIH grants AI072683 (to J.A.C.), AI18697A1 (to R.K.M. and D.H.C.), and AI141801 (to R.T.M. and J.A.C.).

REFERENCES

- Centers for Disease Control and Prevention. 2008. Anaplasma phagocytophilum transmitted through blood transfusion—Minnesota, 2007. MMWR Morb Mortal Wkly Rep 57:1145–1148.
- Alhumaidan H, Westley B, Esteva C, Berardi V, Young C, Sweeney J. 2013. Transfusion-transmitted anaplasmosis from leukoreduced red blood cells. Transfusion 53:181–186. <https://doi.org/10.1111/j.1537-2995.2012.03685.x>.
- Annen K, Friedman K, Eshoa C, Horowitz M, Gottschall J, Straus T. 2012. Two cases of transfusion-transmitted Anaplasma phagocytophilum. Am J Clin Pathol 137:562–565. <https://doi.org/10.1309/AJCP4E4VQQQOZIAQ>.
- Bakken JS, Dumler JS. 2015. Human granulocytic anaplasmosis. Infect Dis Clin North Am 29:341–355. <https://doi.org/10.1016/j.idc.2015.02.007>.
- Bakken JS, Krueth JK, Lund T, Malkovitch D, Asanovich K, Dumler JS. 1996. Exposure to deer blood may be a cause of human granulocytic ehrlichiosis. Clin Infect Dis 23:198. <https://doi.org/10.1093/clinids/23.1.198>.

6. Horowitz HW, Kilchevsky E, Haber S, Agüero-Rosenfeld M, Kranwinkel R, James EK, Wong SJ, Chu F, Liveris D, Schwartz I. 1998. Perinatal transmission of the agent of human granulocytic ehrlichiosis. *N Engl J Med* 339:375–378. <https://doi.org/10.1056/NEJM199808063390604>.
7. Ismail N, McBride JW. 2017. Tick-borne emerging infections: ehrlichiosis and anaplasmosis. *Clin Lab Med* 37:317–340. <https://doi.org/10.1016/j.cll.2017.01.006>.
8. Zhang L, Liu Y, Ni D, Li Q, Yu Y, Yu XJ, Wan K, Li D, Liang G, Jiang X, Jing H, Run J, Luan M, Fu X, Zhang J, Yang W, Wang Y, Dumler JS, Feng Z, Ren J, Xu J. 2008. Nosocomial transmission of human granulocytic anaplasmosis in China. *JAMA* 300:2263–2270. <https://doi.org/10.1001/jama.2008.626>.
9. Bakken JS, Dumler JS. 2006. Clinical diagnosis and treatment of human granulocytotropic anaplasmosis. *Ann N Y Acad Sci* 1078:236–247. <https://doi.org/10.1196/annals.1374.042>.
10. Agüero-Rosenfeld ME, Donnarumma L, Zentmaier L, Jacob J, Frey M, Noto R, Carbonaro CA, Wormser GP. 2002. Seroprevalence of antibodies that react with *Anaplasma phagocytophilum*, the agent of human granulocytic ehrlichiosis, in different populations in Westchester County, New York. *J Clin Microbiol* 40:2612–2615. <https://doi.org/10.1128/jcm.40.7.2612-2615.2002>.
11. Bakken JS, Goellner P, Van Etten M, Boyle DZ, Swonger OL, Mattson S, Krueth J, Tilden RL, Asanovich K, Walls J, Dumler JS. 1998. Seroprevalence of human granulocytic ehrlichiosis among permanent residents of northwestern Wisconsin. *Clin Infect Dis* 27:1491–1496. <https://doi.org/10.1086/515048>.
12. Bakken JS, Krueth J, Wilson-Nordskog C, Tilden RL, Asanovich K, Dumler JS. 1996. Clinical and laboratory characteristics of human granulocytic ehrlichiosis. *JAMA* 275:199–205. <https://doi.org/10.1001/jama.1996.03530270039029>.
13. Belongia EA, Gale CM, Reed KD, Mitchell PD, Vandermause M, Finkel MF, Kazmierczak JJ, Davis JP. 2001. Population-based incidence of human granulocytic ehrlichiosis in northwestern Wisconsin, 1997–1999. *J Infect Dis* 184:1470–1474. <https://doi.org/10.1086/324517>.
14. Dahlgren FS, Mandel EJ, Krebs JW, Massung RF, McQuiston JH. 2011. Increasing incidence of Ehrlichia chaffeensis and Anaplasma phagocytophilum in the United States, 2000–2007. *Am J Trop Med Hyg* 85:124–131. <https://doi.org/10.4269/ajtmh.2011.10.0613>.
15. Leiby DA, Chung AP, Cable RG, Trouern-Trend J, McCullough J, Homer MJ, Reynolds LD, Houghton RL, Lodes MJ, Persing DH. 2002. Relationship between tick bites and the seroprevalence of Babesia microti and Anaplasma phagocytophilum (previously Ehrlichia sp.) in blood donors. *Transfusion* 42:1585–1591. <https://doi.org/10.1046/j.1537-2995.2002.00251.x>.
16. Troese MJ, Carlyon JA. 2009. Anaplasma phagocytophilum dense-cored organisms mediate cellular adherence through recognition of human P-selectin glycoprotein ligand 1. *Infect Immun* 77:4018–4027. <https://doi.org/10.1128/IAI.00527-09>.
17. Kahlon A, Ojogun N, Ragland SA, Seidman D, Troese MJ, Ottens AK, Mastrorunzio JE, Truchan HK, Walker NJ, Borjesson DL, Fikrig E, Carlyon JA. 2013. Anaplasma phagocytophilum Asp14 is an invasin that interacts with mammalian host cells via its C terminus to facilitate infection. *Infect Immun* 81:65–79. <https://doi.org/10.1128/IAI.00932-12>.
18. Ojogun N, Kahlon A, Ragland SA, Troese MJ, Mastrorunzio JE, Walker NJ, Viebrock L, Thomas RJ, Borjesson DL, Fikrig E, Carlyon JA. 2012. Anaplasma phagocytophilum outer membrane protein A interacts with sialylated glycoproteins to promote infection of mammalian host cells. *Infect Immun* 80:3748–3760. <https://doi.org/10.1128/IAI.00654-12>.
19. Seidman D, Ojogun N, Walker NJ, Mastrorunzio J, Kahlon A, Hebert KS, Karandashova S, Miller DP, Tegels BK, Marconi RT, Fikrig E, Borjesson DL, Carlyon JA. 2014. Anaplasma phagocytophilum surface protein AipA mediates invasion of mammalian host cells. *Cell Microbiol* 16:1133–1145. <https://doi.org/10.1111/cmi.12286>.
20. Seidman D, Hebert KS, Truchan HK, Miller DP, Tegels BK, Marconi RT, Carlyon JA. 2015. Essential domains of Anaplasma phagocytophilum invasins utilized to infect mammalian host cells. *PLoS Pathog* 11:e1004669. <https://doi.org/10.1371/journal.ppat.1004669>.
21. Green RS, Naimi WA, Oliver LD, O'Bier N, Cho J, Conrad DH, Martin RK, Marconi RT, Carlyon JA. 2020. Binding of host cell surface protein disulfide isomerase by Anaplasma phagocytophilum Asp14 enables pathogen infection. *mBio* 11:e03141-19. <https://doi.org/10.1128/mBio.03141-19>.
22. Ducken DR, Brown WC, Alperin DC, Brayton KA, Reif KE, Turse JE, Palmer GH, Noh SM. 2015. Subdominant outer membrane antigens in Anaplasma marginale: conservation, antigenicity, and protective capacity using recombinant protein. *PLoS One* 10:e0129309. <https://doi.org/10.1371/journal.pone.0129309>.
23. Palmer GH, Brown WC, Noh SM, Brayton KA. 2012. Genome-wide screening and identification of antigens for rickettsial vaccine development. *FEMS Immunol Med Microbiol* 64:115–119. <https://doi.org/10.1111/j.1574-695X.2011.00878.x>.
24. Joller N, Weber SS, Muller AJ, Sporri R, Selchow P, Sander P, Hilbi H, Oxenius A. 2010. Antibodies protect against intracellular bacteria by Fc receptor-mediated lysosomal targeting. *Proc Natl Acad Sci U S A* 107:20441–20446. <https://doi.org/10.1073/pnas.1013827107>.
25. Akkoyunlu M, Fikrig E. 2000. Gamma interferon dominates the murine cytokine response to the agent of human granulocytic ehrlichiosis and helps to control the degree of early rickettsemia. *Infect Immun* 68:1827–1833. <https://doi.org/10.1128/iai.68.4.1827-1833.2000>.
26. Birkner K, Steiner B, Rinkler C, Kern Y, Aichele P, Bogdan C, von Loewenich FD. 2008. The elimination of Anaplasma phagocytophilum requires CD4+ T cells, but is independent of Th1 cytokines and a wide spectrum of effector mechanisms. *Eur J Immunol* 38:3395–3410. <https://doi.org/10.1002/eji.200838615>.
27. Martin ME, Caspersen K, Dumler JS. 2001. Immunopathology and ehrlichial propagation are regulated by interferon-gamma and interleukin-10 in a murine model of human granulocytic ehrlichiosis. *Am J Pathol* 158:1881–1888. [https://doi.org/10.1016/S0002-9440\(10\)64145-4](https://doi.org/10.1016/S0002-9440(10)64145-4).
28. Scorpio DG, von Loewenich FD, Gobel H, Bogdan C, Dumler JS. 2006. Innate immune response to Anaplasma phagocytophilum contributes to hepatic injury. *Clin Vaccine Immunol* 13:806–809. <https://doi.org/10.1128/CVI.00092-06>.
29. Walker DH, Dumler JS. 2015. The role of CD8 T lymphocytes in rickettsial infections. *Semin Immunopathol* 37:289–299. <https://doi.org/10.1007/s00281-015-0480-x>.
30. Dumler JS. 2012. The biological basis of severe outcomes in Anaplasma phagocytophilum infection. *FEMS Immunol Med Microbiol* 64:13–20. <https://doi.org/10.1111/j.1574-695X.2011.00909.x>.
31. Scorpio DG, Choi KS, Dumler JS. 2018. Anaplasma phagocytophilum-related defects in CD8, NKT, and NK lymphocyte cytotoxicity. *Front Immunol* 9:710. <https://doi.org/10.3389/fimmu.2018.00710>.
32. Cain DW, Sanders SE, Cunningham MM, Kelsoe G. 2013. Disparate adjuvant properties among three formulations of “alum.” *Vaccine* 31:653–660. <https://doi.org/10.1016/j.vaccine.2012.11.044>.
33. Earnhart CG, Buckles EL, Dumler JS, Marconi RT. 2005. Demonstration of OspC type diversity in invasive human Lyme disease isolates and identification of previously uncharacterized epitopes that define the specificity of the OspC murine antibody response. *Infect Immun* 73:7869–7877. <https://doi.org/10.1128/IAI.73.12.7869-7877.2005>.
34. Earnhart CG, Leblanc DV, Alix KE, Desrosiers JC, Radolf JD, Marconi RT. 2010. Identification of residues within ligand-binding domain 1 (LBD1) of the Borrelia burgdorferi OspC protein required for function in the mammalian environment. *Mol Microbiol* 76:393–408. <https://doi.org/10.1111/j.1365-2958.2010.07103.x>.
35. Earnhart CG, Marconi RT. 2007. OspC phylogenetic analyses support the feasibility of a broadly protective polyvalent chimeric Lyme disease vaccine. *Clin Vaccine Immunol* 14:628–634. <https://doi.org/10.1128/CVI.00409-06>.
36. Earnhart CG, Marconi RT. 2007. An octavalent Lyme disease vaccine induces antibodies that recognize all incorporated ospC type-specific sequences. *Hum Vaccin* 3:281–289. <https://doi.org/10.4161/hv.4661>.
37. Izac JR, O'Bier NS, Oliver LD, Jr, Camire AC, Earnhart CG, LeBlanc Rhodes DV, Young BF, Parnham SR, Davies C, Marconi RT. 2020. Development and optimization of OspC chimeritope vaccinogens for Lyme disease. *Vaccine* 38:1915–1924. <https://doi.org/10.1016/j.vaccine.2020.01.027>.
38. Oliver LD, Jr, Earnhart CG, Virginia-Rhodes D, Theisen M, Marconi RT. 2016. Antibody profiling of canine IgG responses to the OspC protein of the Lyme disease spirochetes supports a multivalent approach in vaccine and diagnostic assay development. *Vet J* 218:27–33. <https://doi.org/10.1016/j.tvjl.2016.11.001>.
39. Browning MD, Garyu JW, Dumler JS, Scorpio DG. 2006. Role of reactive nitrogen species in development of hepatic injury in a C57Bl/6 mouse model of human granulocytic anaplasmosis. *Comp Med* 56:55–62.
40. Martin ME, Bunnell JE, Dumler JS. 2000. Pathology, immunohistology, and cytokine responses in early phases of human granulocytic ehrlichiosis in a murine model. *J Infect Dis* 181:374–378. <https://doi.org/10.1086/315206>.
41. Scorpio DG, Von Loewenich FD, Bogdan C, Dumler JS. 2005. Innate immune tissue injury and murine HGA: tissue injury in the murine model of granulocytic anaplasmosis relates to host innate immune response

- and not pathogen load. *Ann N Y Acad Sci* 1063:425–428. <https://doi.org/10.1196/annals.1355.077>.
42. von Loewenich FD, Scorpio DG, Reischl U, Dumler JS, Bogdan C. 2004. Frontline: control of *Anaplasma phagocytophilum*, an obligate intracellular pathogen, in the absence of inducible nitric oxide synthase, phagocyte NADPH oxidase, tumor necrosis factor, Toll-like receptor (TLR)2 and TLR4, or the TLR adaptor molecule MyD88. *Eur J Immunol* 34:1789–1797. <https://doi.org/10.1002/eji.200425029>.
 43. Cockburn CL, Green RS, Damle SR, Martin RK, Ghahrai NN, Colonne PM, Fullerton MS, Conrad DH, Chalfant CE, Voth DE, Rucks EA, Gilk SD, Carlyon JA. 2019. Functional inhibition of acid sphingomyelinase disrupts infection by intracellular bacterial pathogens. *Life Sci Alliance* 2:e201800292. <https://doi.org/10.26508/lsa.201800292>.
 44. Naimi WA, Green RS, Cockburn CL, Carlyon JA. 2018. Differential susceptibility of male versus female laboratory mice to *Anaplasma phagocytophilum* infection. *Trop Med Infect Dis* 3:78. <https://doi.org/10.3390/tropicalmed3030078>.
 45. Cooper HM, Paterson Y. 2009. Production of polyclonal antisera. *Curr Protoc Neurosci Chapter 5:Unit 5.5*. <https://doi.org/10.1002/0471142301.ns0505s48>.
 46. Oki AT, Huang B, Beyer AR, May LJ, Truchan HK, Walker NJ, Galloway NL, Borjesson DL, Carlyon JA. 2016. *Anaplasma phagocytophilum* APH0032 is exposed on the cytosolic face of the pathogen-occupied vacuole and co-opts host cell SUMOylation. *Front Cell Infect Microbiol* 6:108. <https://doi.org/10.3389/fcimb.2016.00108>.
 47. Livak KJ, Schmittgen TD. 2001. Analysis of relative gene expression data using real-time quantitative PCR and the 2^{-ΔΔC_T} method. *Methods* 25:402–408. <https://doi.org/10.1006/meth.2001.1262>.
 48. Huang B, Hubber A, McDonough JA, Roy CR, Scidmore MA, Carlyon JA. 2010. The *Anaplasma phagocytophilum*-occupied vacuole selectively recruits Rab-GTPases that are predominantly associated with recycling endosomes. *Cell Microbiol* 12:1292–1307. <https://doi.org/10.1111/j.1462-5822.2010.01468.x>.